Letter

Fate of the upper polariton: Breakdown of the quasiparticle picture in the continuum

Yesenia A. García Jomaso, Brenda Vargas, David Ley Dominguez, César L. Ordoñez-Romero, Hugo A. Lara-García, Arturo Camacho-Guardian,* and Giuseppe Pirruccio†

Instituto de Física, Universidad Nacional Autónoma de México, Ciudad de México CP 04510, Mexico

(Received 30 September 2022; revised 10 February 2023; accepted 16 February 2023; published 27 February 2023)

Organic polaritons, strongly hybridized light-matter excitations, have arisen as a platform to device optical interfaces at room temperature. Despite their inherent complexity, polaritons are commonly regarded as coherent excitations described by Landau's quasiparticle theory. Here, we theoretically study and experimentally demonstrate the role of incoherent matter excitations in terms of generalized Hopfield coefficients, which unveil the fading of the upper polariton at its entrance to a continuum of molecular excitations. This marks the breakdown of the simplistic quasiparticle picture and the formation of a more complex quantum state beyond Landau's formalism.

DOI: 10.1103/PhysRevB.107.L081302

Introduction. Coherent phenomena generally benefit from the lack of noise [1–3]. Isolation from the environment helps in removing external sources of decoherence and it is routinely applied in quantum technologies: quantum optics [4], quantum computing [5,6], and cryptography [7,8]. However, this strategy is ineffective against noise arising from internal processes that cannot be disentangled from the system under research. Conversely to what it is typically thought, noise is not always detrimental and can drive unexpected phenomena at all scales [9–12]. At the nanoscale, the presence of noise or disorder in complex systems gives rise to random lasers [13–15], Anderson localization [16], and enhanced energy transport [17]. Stochastic resonances [18], the Purcell effect [19], Casimir forces [20], and radiative heat transfer [21,22] are other important manifestations of noise-driven physics. Frequency noise is epitomized by the broadening of a resonance linewidth. Even though only white noise truly embodies a continuum, a sufficiently wide frequency window of available competing states effectively plays the role of a continuum.

A novel and intriguing class of coherent excitations is cavity polaritons, which result from the strong coupling between confined photons and matter excitations [23,24]. Polaritons are usually described within Landau's quasiparticle theory, which stands nowadays as one of the most powerful concepts in physics [25–27]. Describing the linear hybridization of light and matter in terms of polaritons reduces dramatically the complexity of the system. The realm of Landau's theory extends to interactions and allows for the study of effective photon-photon interactions [28–31]. Dressed by its environments, a new quasiparticle coined the polaron-polariton can also summarize the many-body complexity of the system [32–36]. However, intrinsic or extrinsic processes can lead to the breakdown of the polariton picture where their description can no longer be captured by the quasiparticle properties. Organic polaritons feature complicated processes as a result of the large number of internal degrees of freedom [37–41]. Understanding the extent of the quasiparticle theory remains as an experimental and theoretical challenge in these systems.

Motivated by the rapid progress and the necessity to deepen the understanding of organic polaritons, in this Letter we propose a strongly coupled optical cavity embedding a dye-doped polymer as a paradigmatic platform to experimentally explore the range of validity of Landau's quasiparticle theory in the presence of a continuum of matter excitations. Our results can be readily extrapolated to other scenarios where a continuum of states competes with coherent excitations. By combining a general field theory and experimental observations, we study the validity and breakdown of the ideal polariton picture in terms of generalized Hopfield coefficients and unravel the role of the continuum on the quasiparticle properties of exciton-polaritons. The experimental control of the energy and momentum of the polaritons allows us to gradually tune one of the polariton branches inside the matter continuum which represents a way to directly visualize the breakdown of the quasiparticle properties of the upper polariton. Despite that the importance of the exciton continuum on the spectrum of organic polaritons has already been recognized, the quantitative characterization of such effects in terms of their quasiparticle properties remains pending. The introduction of the generalized Hopfield coefficients and the experimental demonstration of their validity constitute our main result. We anticipate that the breakdown of the quasiparticle picture may have important consequences on the polariton ultrafast dynamics which is intimately related to important cavity-mediated phenomena already observed, such as condensation [42,43], polariton chemistry [44], singlet fission [45], vibrational strong coupling [46], ultrastrong coupling [47,48], and temperature-activated delayed fluorescence and phosphorescence [49].

System. Our nanocavity consists of two Ag mirrors sandwiching a thin active layer of ErB molecules embedded in a polyvinyl alcohol (PVA) matrix. A 0.5 M concentration of ErB ensures the system is in the strong light-matter coupling

*acamacho@fisica.unam.mx
†pirruccio@fisica.unam.mx

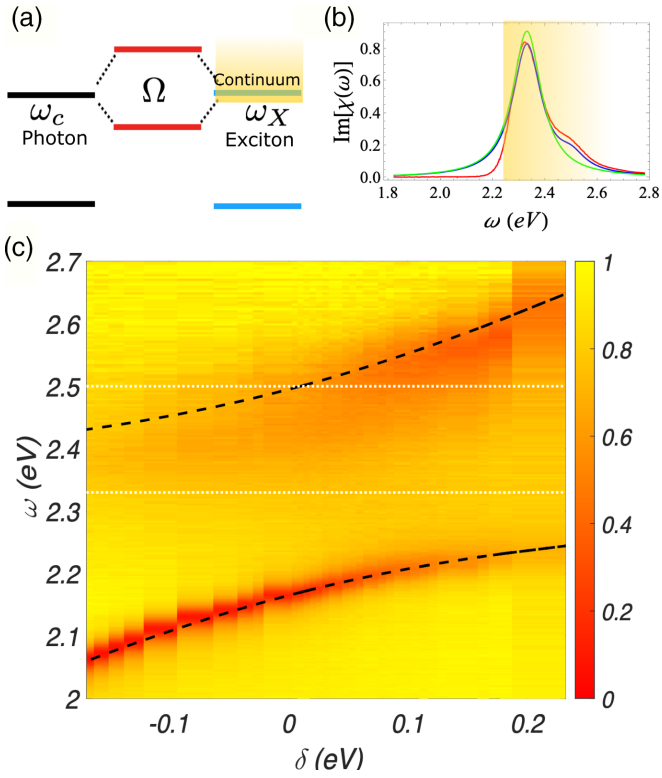

FIG. 1. (a) Simplified energy diagrams for the photon and exciton fields, the latter being embedded in a nondispersive continuum of incoherent excitations. (b) Measured absorption spectrum of the active layer expressed as $\mathrm{Im}[\chi(\omega)]$ (red curve). Blue curve corresponds to the theoretical modeling of the absorption, while the green one to that of a single exciton peak with a standard broadening γ_X. (c) Experimental reflectance spectra at normal incidence as a function of the cavity detuning. Dashed black lines correspond to the LP and UP energies while the white lines are guidelines for the continuum broadening of the Frenkel exciton.

regime. The cavity is fabricated by first sputtering a Ag mirror of thickness 300 nm on top of a glass substrate. The active layer of nominal thickness L_c is deposited by spin coating and, finally, a second Ag mirror of thickness 25 nm is sputtered on top of it. For all practical means, the first mirror can be treated as semi-infinite. L_c is chosen such that the energy of the fundamental cavity mode lies close to the exciton one; i.e., L_c is around 160 nm depending on the cavity detuning to be studied.

The optical response of the active medium can be described by its optical susceptibility $\chi(\omega)$. The absorption of the layer, captured by $\mathrm{Im}\chi(\omega)$, is illustrated with a red curve in Fig. 1(b) (see [50]). The absorption spectrum exhibits nontrivial features associated with vibrational bands, exciton interactions, and anisotropies, among others [51]. It consists of the main peak centered at $\omega_X \approx 2.33$ eV associated with the principal $S_0 \rightarrow S_1$ transition and an overlapping second mode that gives rise to a bump close to $\omega \approx 2.5$ eV. The nontrivial broadening of both results in a continuous range of excitations, which we simply refer to as *incoherent matter continuum* [see Fig. 1(b)]. Rather than focusing on its microscopic origin, which lies beyond the scope of this Letter, here we unveil the effects of this nondispersive incoherent continuum on the quasiparticle character of the exciton-polaritons.

Cavity polaritons. The collective coupling of the organic molecules to the fundamental cavity mode give rises to two quasiparticle branches coined lower (LP) and upper (UP) polaritons. The energy of these states is given by [52]

$$\omega_{\mathrm{UP/LP}}(\mathbf{k}) = \tfrac{1}{2}(\omega_c(\mathbf{k}) + \omega_X \pm \sqrt{[\omega_c(\mathbf{k}) - \omega_X]^2 + 4\Omega^2}). \tag{1}$$

Here, the dispersion $\omega_c(\mathbf{k}) = \frac{c}{n_c}\sqrt{k_z^2 + k_{||}^2}$ represents a continuum of photonic states. We take the incident light along the z axis, perpendicular to the cavity mirrors, with an angle θ, that is $k_{||} = n_c \frac{\omega}{c} \sin\theta$. The collective coupling of the molecules to light is characterized by the Rabi splitting $\Omega = \sqrt{n}g$, expressed in terms of the coupling between a single molecule and a cavity photon g, enhanced by the number of molecules. Finally, we introduce the cavity energy detuning from the exciton $\delta(\mathbf{k}) = \omega_c(\mathbf{k}) - \omega_X$.

By combining energy-momentum microscopy with a slow linear gradient in the active layer thickness we are able to set the energy of the cavity across a wide range that encompasses all relevant detunings (see [50]). Figure 1(c) displays the measured normal incidence reflectance spectrum for varying $\delta = \delta(\mathbf{k} = 0)$. We observe the appearance of two polariton branches characterized by an avoided crossing with a Rabi coupling of $2\Omega = 0.34$ eV. Here the dashed black curves give the energy of the polariton branches in Eq. (1). We estimate a broadening of the cavity photons of $\gamma_c \approx 0.05$ eV, and the Lorentzian broadening of the excitons of $\gamma_X \approx 0.065$ eV. Being $2\Omega \gg \gamma_X, \gamma_c$, our system is in the strongly interacting regime of light and matter.

Figure 1(c) demonstrates the emergence of two polariton branches exhibiting a striking difference. The LP arises and maintains its well-defined quasiparticle character as the cavity detuning is varied from mostly photonic ($\delta < 0$) to excitonic ($\delta > 0$). Although the reflectance reduces for large positive detunings, the LP branch remains well defined and can be interpreted as an ideal polariton, accurately described by Eq. (1).

The UP, in contrast, exhibits a more intriguing behavior. For large and positive δ, a well-defined polariton state emerges with energy in good agreement with Eq. (1). Interestingly, as the detuning decreases, the UP becomes blurred until no clear signature of this branch can be identified. Although we expect the signal of the UP to weaken as it evolves from photonic to excitonic, we observe its fading even at maximal mixing ($\delta = 0$), which strongly contrasts with the signal of the LP. Contrary to the ideal polaritons that are symmetric at $\delta = 0$, the asymmetric line shape of the exciton absorption makes the UP and LP highly asymmetric.

The intricate features of the UP can intuitively be understood as follows: The absorption spectrum in Fig. 1(b) exhibits a mean exciton peak and a complex enveloping matter continuum for energies larger than that of the bare exciton. Thus, the simple two-level diagram of the exciton acquires a more complex structure, as sketched in Fig. 1(a). Coupled to a cavity, the Frenkel excitons hybridize with photons yielding two polariton branches that repel each other in energy. The LP is located at energies lower than the bare exciton one, ω_X, and, thus, it is always pushed away from the matter continuum

[see Fig. 1(a)]. Conversely, the UP lies at energies larger than ω_X. Thus, depending on the cavity detuning, it can be placed within the matter continuum. In Fig. 1(c) we signal the matter continuum with dashed white lines, which help in noticing that when the polaritons are driven from large positive to negative detunings, the UP vanishes gradually at its entrance in the continuum. When it lies inside the continuum, it is no longer possible to identify a well-defined polariton, marking the breakdown of the quasiparticle picture. We stress that the white lines in Fig. 1(c) are a guide to specify in which range the polariton is ill defined. However, this is a crossover rather than a sharp transition; that is, the UP evolves smoothly to a well-defined quasiparticle as its energy departs from the continuum.

Landau's quasiparticle theory allows summarizing a complex many-body system into a few single-particle properties [27]. Here, we employ a field-theoretical approach which permits the study of polaritons within a general theoretical framework. Let us introduce $\hat{x}^\dagger$ and $\hat{c}^\dagger$ the operators that create an exciton and a photon, respectively. The imaginary-time Green's function [53]

$$\mathcal{G}_{\alpha,\beta}(\mathbf{k},\tau) = -\langle T_\tau\{\hat{\psi}_\alpha(\tau)\hat{\psi}^\dagger_\beta(0)\}\rangle, \tag{2}$$

defined as a matrix, where the indices $\alpha,\beta = \{c,x\}$ give the photon $[\psi^\dagger_c(\tau) = \hat{c}^\dagger(\tau)]$ and exciton $[\psi^\dagger_x(\tau) = \hat{x}^\dagger(\tau)]$ field operators and T_τ is the time-ordering operator. Here, we have made the dependence on the incident wave vector, $\mathbf{k}$, explicit.

The dynamics of the matrix Green's function is governed by a Dyson equation

$$\mathcal{G}^{-1}_{\alpha,\beta}(\mathbf{k},\omega) = \left[G^{(0)}_{\alpha,\beta}(\mathbf{k},\omega)\right]^{-1} - \Sigma_{\alpha,\beta}(\mathbf{k},\omega),$$

where $G^{(0)}_{\alpha,\beta}(\mathbf{k},\omega)$ denotes the ideal photonic and excitonic Green's function and it reads as $[G^{(0)}_{\alpha,\beta}(\mathbf{k},\omega)]^{-1} = \mathrm{diag}[\omega-\omega_c(\mathbf{k}),\omega-\omega_X]$. The off-diagonal terms of the self-energy, $\Sigma_{\alpha,\beta}(\mathbf{k},\omega)$, are determined by the light-matter coupling $\Sigma_{cx}(\mathbf{k},\omega) = \Sigma_{xc}(\mathbf{k},\omega) = \Omega$, whereas the diagonal term $\Sigma_{xx}(\mathbf{k},\omega)$ describes the incoherent part of the excitonic spectrum. The polariton energies are calculated by the real poles of the dressed Green's function $\mathrm{Re}[\mathcal{G}^{-1}_{xx}(\mathbf{k},\omega)] = 0$ that account for the light-matter coupling and the matter continuum. In absence of the decoherence processes, this equation determines the standard UP/LP polariton energies in Eq. (1).

In addition to their energies, quasiparticles are defined by their residue, which accounts for the overlap between the bare and dressed states. In our formalism, the residues are given by

$$Z_{\mathrm{LP(UP)}}(\mathbf{k}) = \left(\frac{\partial \mathrm{Re}\left[\mathcal{G}^{-1}_{xx}(\mathbf{k},\omega)\right]}{\partial\omega}\right)^{-1}\Bigg|_{\omega=\omega_{\mathrm{LP(UP)}}(\mathbf{k})}. \tag{3}$$

Within Landau's quasiparticle theory $0 < Z_{\mathrm{LP(UP)}}(\mathbf{k}) \leqslant 1$. In the absence of interactions, a polariton can be regarded as a coherent superposition of a photon and an exciton; in this case, the residue of the quasiparticle is directly connected to the Hopfield coefficients $Z_{\mathrm{LP(UP)}}(\mathbf{k}) = \mathcal{C}^2_{\mathbf{k}}$ $(\mathcal{S}^2_{\mathbf{k}})$. Ideal polaritons retain all the spectral weight in the form of coherent excitations, that is, $Z_{\mathrm{LP}}(\mathbf{k}) + Z_{\mathrm{UP}}(\mathbf{k}) = \mathcal{C}^2_{\mathbf{k}} + \mathcal{S}^2_{\mathbf{k}} = 1$ with $\mathcal{C}^2_{\mathbf{k}} = \frac{1}{2}\left(1 + \frac{\delta(\mathbf{k})}{\sqrt{\delta^2(\mathbf{k})+4\Omega^2}}\right)$.

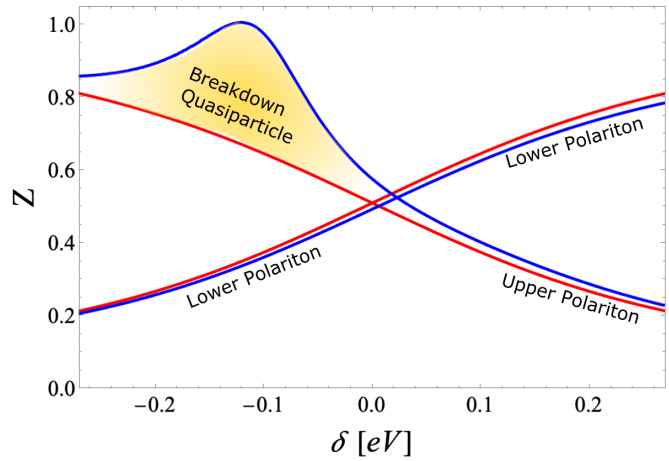

FIG. 2. Quasiparticle residue of the polariton branches calculated at normal incidence. Red curves correspond to ideal polaritons, while blue ones denote the generalized Hopfield coefficients. The yellow area depicts the deviation from the ideal UP and illustrates the breakdown of the quasiparticle picture for this branch.

Our general formalism allows us to explore physics beyond the ideal polaritons. Here, we employ a phenomenological model that closely resembles the experimental absorption in Fig. 1(b) (blue curve). Our model contemplates the principal exciton, a weak coupling to a second mode, and Lorentzian broadening of the excitonic and photonic lines as detailed in the Supplemental Material [50]. We start by looking into the residue of the quasiparticle. This defines generalized Hopfield coefficients that may differ from the ideal theory. This is the main result of our Letter and is illustrated in Fig. 2 where we show the ideal (red curves) and generalized Hopfield coefficients (blue curves) for the UP and LP. Our theoretical approach obeys the sum rule $1 = \int \frac{d\omega}{2\pi} A_{xx}(\mathbf{k},\omega)$, with $A_{xx}(\mathbf{k},\omega) = -2\mathrm{Im}\mathcal{G}_{xx}(\mathbf{k},\omega)$, which implies that the spectral weight is always preserved. For large positive and negative detuning, the generalized Hopfield coefficients asymptotically lead to well defined quasiparticles for both branches as the matter and light decouple leading to the bare exciton and photon branches. Moreover, the LP is well described by the ideal theory, for all detunings. Intriguingly, as the detuning is varied from positive to negative values, we start noticing a stark disagreement between the ideal and generalized Hopfield for the UP. The associated residue increases and approaches $Z_{\mathrm{UP}}(\mathbf{k}) \sim 1$, leading to an unphysical value of $Z_{\mathrm{LP}}(\mathbf{k}) + Z_{\mathrm{UP}}(\mathbf{k}) > 1$ and, thus, indicating the failing of the quasiparticle approach to describe the UP. We stress that the spectral function remains always normalized for all values of the detuning. The shaded yellow area in Fig. 2 corresponds to the regime where the sum rule is conserved but the high-energy branch can no longer be understood as a quasiparticle.

In Fig. 2 we have added a broadening to the exciton line equal to $\gamma_X = 0.065$ eV, which corresponds to the absorption spectrum in Fig. 1(b) (green curve). This indicates that homogeneous broadening of the exciton absorption in general does not suffice to break the quasiparticle picture.

To further understand the limits of the quasiparticle picture, we now investigate the dispersion of the polariton branches as a function of the in-plane wave vector, $k_{||}$, and for three

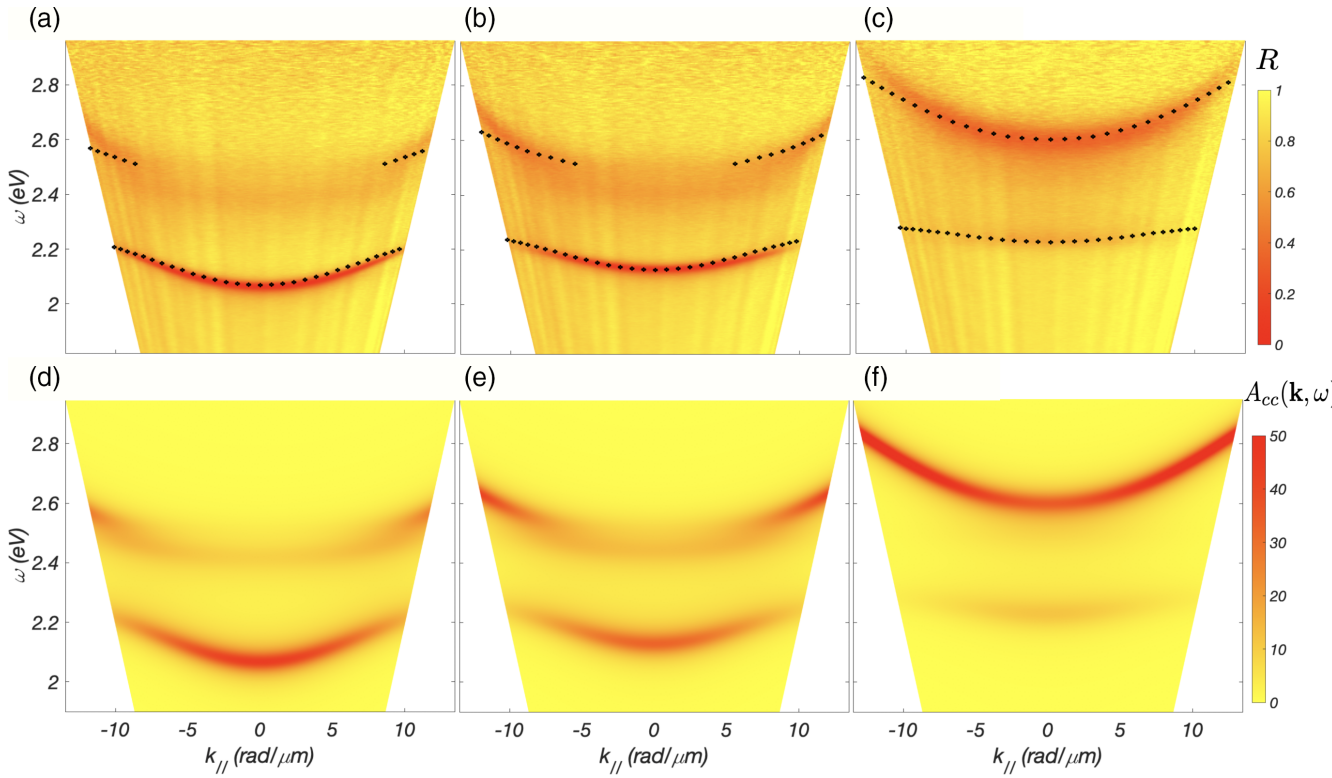

FIG. 3. Top: Experimental *s*-polarized reflectance as a function of the in-plane momentum, $k_{||}$, for several values of the detuning, δ. (a) Negative detuning $\delta = -0.18$ eV, (b) close to maximal mixing $\delta = -0.07$ eV, and (c) positive detuning $\delta = 0.15$ eV. The black squares denote the polariton energies obtained from the field theory. Bottom: Spectral function of the cavity field for the same parameters as the experiment.

values of the detuning. For $\delta = -0.18$ eV, shown in Fig. 3(a), we observe a single well-defined low-energy polariton branch and a blurred region at higher energies. Here, the LP arises far from the matter continuum and remains clearly visible for all measured in-plane momentum. The remnant of the UP appears as a foggy region where the reflectance drops. For large values of $k_{||}$, the signatures of the UP are slightly more visible. Here, the black squares correspond to the quasiparticle energies obtained from our field theory. Squares are plotted only in the regions of the dispersion diagram where the ideal quasiparticle picture provides physical results. The success of our extended theory is evident from the excellent agreement found between our measurements and the spectral function of the photon field, $A_{cc}(\mathbf{k},\omega) = -2\mathrm{Im}\mathcal{G}_{cc}(\mathbf{k},\omega)$, plotted in Fig. 3(d).

With increasing δ, as shown for $\delta = -0.07$ eV in Fig. 3(b), the LP retains its visibility, whereas the UP remains blurred for small wave vectors and gains coherence for larger ones. This can be understood intuitively: for small wave vectors the polariton is formed predominantly by matter and strongly influenced by the matter continuum. On the contrary, with increasing wave vector the polariton exits the continuum and its linewidth narrows as a consequence of a dominant photonic component [50]. Here again, we find a very good agreement with our theoretical approach as shown in Fig. 3(e).

Finally, in Fig. 3(c) we see the emergence of a well-defined UP for positive detuning, $\delta = 0.15$ eV, and for all $k_{||}$, with a very good agreement with the theory shown in Fig. 3(f). This is consistent with Fig. 1(c) and with our previous discussion. The LP, on the other hand, exhibits an increased reflectance and loses spectral weight. However, the lower visibility of the LP is a consequence of the small photonic component rather than a breakdown of the quasiparticle picture for this branch since the matter continuum lies above its energy, as shown in Fig. 1.

Conclusions and outlook. Exciton-polaritons provide a simple yet very powerful description of hybrid light-matter systems which have proven to be extremely successful to approach a plethora of systems within the linear and nonlinear regimes. In this work, we have experimentally and theoretically studied the validity of Landau's quasiparticle theory for organic molecules strongly coupled to cavity photons at room temperature. By varying the cavity photon energy-momentum we controlled the quasiparticle nature of the upper polariton, revealing that the paling and broadening of the corresponding branch at its entrance to the continuum is a consequence of ill-defined generalized Hopfield coefficients. The inability to associate physical Hopfield coefficients to this branch marks the breakdown of the single-polariton picture. Our general theoretical framework expands the study of exciton-polaritons beyond Landau's theory and agrees remarkably well with the experiment. This formalism is well suited for other organic and inorganic polariton systems.

Complex intrinsic and/or extrinsic processes are, in general, features that cannot be disentangled from coherent excitations and can render the quasiparticle picture invalid. These sources of decoherence are not necessarily detrimental, but their role can be exploited as a mechanism to detect, probe, and control underlying complicated processes and further be employed to tailor many-body phenomena beyond quasiparticle physics. Finally, their presence may play an important role in the temporal dynamics, scattering thermalization, and relaxation of organic exciton-polaritons. Despite being commonly disregarded, the understanding of many-body interactions, as the ones discussed in this Letter, is paramount for advancing the organic polariton research field.

Acknowledgments. G.P. acknowledges financial support from UNAM DGAPA PAPIIT Grant No. IN104522 and CONACyT Projects No. 1564464 and No. 1098652. H.L.G. acknowledges financial support from UNAM DGAPA PAPIIT Grants No. IA103621 and No. IA107023. A.C.G. acknowledges financial support from UNAM DGAPA PAPIIT Grants No. IN108620 and No. IA101923. C.L.O.-R. acknowledges financial support from UNAM DGAPA PAPIIT Grant No. IG100521.

[1] W. H. Zurek, Rev. Mod. Phys. **75**, 715 (2003).
[2] H. Rabitz, R. de Vivie-Riedle, M. Motzkus, and K. Kompa, Science **288**, 824 (2000).
[3] L. Viola, E. Knill, and S. Lloyd, Phys. Rev. Lett. **82**, 2417 (1999).
[4] M. Orszag, *Quantum Optics: Including Noise Reduction, Trapped Ions, Quantum Trajectories, and Decoherence* (Springer, Berlin, Germany, 2016).
[5] R. Alicki, M. Horodecki, P. Horodecki, and R. Horodecki, Phys. Rev. A **65**, 062101 (2002).
[6] R. Horodecki, P. Horodecki, M. Horodecki, and K. Horodecki, Rev. Mod. Phys. **81**, 865 (2009).
[7] N. Gisin, G. Ribordy, W. Tittel, and H. Zbinden, Rev. Mod. Phys. **74**, 145 (2002).
[8] T. C. Ralph, Phys. Rev. A **61**, 010303(R) (1999).
[9] R. de J. León-Montiel and J. P. Torres, Phys. Rev. Lett. **110**, 218101 (2013).
[10] S. Viciani, M. Lima, M. Bellini, and F. Caruso, Phys. Rev. Lett. **115**, 083601 (2015).
[11] R. de J. León-Montiel and P. A. Quinto-Su, Sci. Rep. **7**, 44287 (2017).
[12] J. Foldager, A. Pesah, and L. K. Hansen, Sci. Rep. **12**, 3862 (2022).
[13] M. P. Van Albada and A. Lagendijk, Phys. Rev. Lett. **55**, 2692 (1985).
[14] S. John, Phys. Rev. Lett. **58**, 2486 (1987).
[15] N. M. Lawandy, R. M. Balachandran, A. S. L. Gomes, and E. Sauvain, Nature (London) **368**, 436 (1994).
[16] P. W. Anderson, Phys. Rev. **109**, 1492 (1958).
[17] W. Long, Q.-f. Sun, and J. Wang, Phys. Rev. Lett. **101**, 166806 (2008).
[18] L. Gammaitoni, P. Hänggi, P. Jung, and F. Marchesoni, Rev. Mod. Phys. **70**, 223 (1998).
[19] E. M. Purcell, H. C. Torrey, and R. V. Pound, Phys. Rev. **69**, 37 (1946).
[20] H. B. G. Casimir and D. Polder, Phys. Rev. **73**, 360 (1948).
[21] D. Polder and M. Van Hove, Phys. Rev. B **4**, 3303 (1971).
[22] S.-A. Biehs, R. Messina, P. S. Venkataram, A. W. Rodriguez, J. C. Cuevas, and P. Ben-Abdallah, Rev. Mod. Phys. **93**, 025009 (2021).
[23] J. J. Hopfield, Phys. Rev. **112**, 1555 (1958).
[24] S. Pekar, J. Phys. Chem. Solids **5**, 11 (1958).
[25] L. D. Landau, Zh. Eksp. Teor. Fiz. **30**, 1058 (1956).
[26] *Collected Papers of L. D. Landau*, edited by D. ter Haar (Pergamon, 1965), pp. 731–741.
[27] G. Baym and C. Pethick, *Landau Fermi-Liquid Theory: Concepts and Applications* (John Wiley and Sons, Federal Republic of Germany, 1991).
[28] M. Vladimirova, S. Cronenberger, D. Scalbert, K. V. Kavokin, A. Miard, A. Lemaître, J. Bloch, D. Solnyshkov, G. Malpuech, and A. V. Kavokin, Phys. Rev. B **82**, 075301 (2010).
[29] N. Takemura, S. Trebaol, M. Wouters, M. T. Portella-Oberli, and B. Deveaud, Nat. Phys. **10**, 500 (2014).
[30] L. B. Tan, O. Cotlet, A. Bergschneider, R. Schmidt, P. Back, Y. Shimazaki, M. Kroner, and A. İmamoğlu, Phys. Rev. X **10**, 021011 (2020).
[31] I. Schwartz, Y. Shimazaki, C. Kuhlenkamp, K. Watanabe, T. Taniguchi, M. Kroner, and A. Imamoğlu, Science **374**, 336 (2021).
[32] M. Sidler, P. Back, O. Cotlet, A. Srivastava, T. Fink, M. Kroner, E. Demler, and A. Imamoglu, Nat. Phys. **13**, 255 (2017).
[33] J. Levinsen, F. M. Marchetti, J. Keeling, and M. M. Parish, Phys. Rev. Lett. **123**, 266401 (2019).
[34] M. Navadeh-Toupchi, N. Takemura, M. D. Anderson, D. Y. Oberli, and M. T. Portella-Oberli, Phys. Rev. Lett. **122**, 047402 (2019).
[35] M. A. Bastarrachea-Magnani, A. Camacho-Guardian, M. Wouters, and G. M. Bruun, Phys. Rev. B **100**, 195301 (2019).
[36] R. P. A. Emmanuele, M. Sich, O. Kyriienko, V. Shahnazaryan, F. Withers, A. Catanzaro, P. M. Walker, F. A. Benimetskiy, M. S. Skolnick, A. I. Tartakovskii, I. A. Shelykh, and D. N. Krizhanovskii, Nat. Commun. **11**, 3589 (2020).
[37] S. Kéna-Cohen, M. Davanço, and S. R. Forrest, Phys. Rev. Lett. **101**, 116401 (2008).
[38] F. Herrera and F. C. Spano, Phys. Rev. Lett. **118**, 223601 (2017).
[39] J. Keeling and S. Kéna-Cohen, Annu. Rev. Phys. Chem. **71**, 435 (2020).
[40] B. Liu, V. M. Menon, and M. Y. Sfeir, ACS Photonics **7**, 2292 (2020).
[41] M. Sánchez-Barquilla, A. I. Fernández-Domínguez, J. Feist, and F. J. García-Vidal, ACS Photonics **9**, 1830 (2022).
[42] J. D. Plumhof, T. Stöferle, L. Mai, U. Scherf, and R. F. Mahrt, Nat. Mater. **13**, 247 (2014).
[43] K. S. Daskalakis, S. A. Maier, R. Murray, and S. Kéna-Cohen, Nat. Mater. **13**, 271 (2014).
[44] R. F. Ribeiro, L. A. Martínez-Martínez, M. Du, J. Campos-Gonzalez-Angulo, and J. Yuen-Zhou, Chem. Sci. **9**, 6325 (2018).

[45] M. B. Smith and J. Michl, Chem. Rev. **110**, 6891 (2010).
[46] A. Thomas, J. George, A. Shalabney, M. Dryzhakov, S. J. Varma, J. Moran, T. Chervy, X. Zhong, E. Devaux, C. Genet, J. A. Hutchison, and T. W. Ebbesen, Angew. Chem., Int. Ed. **55**, 11462 (2016).
[47] M. Wang, S. Mallick, A. F. Kockum, and K. Börjesson, Phys. Rev. Res. **4**, 023016 (2022).
[48] A. Genco, A. Ridolfo, S. Savasta, S. Patanè, G. Gigli, and M. Mazzeo, Adv. Opt. Mater. **6**, 1800364 (2018).
[49] K. Stranius, M. Hertzog, and K. Börjesson, Nat. Commun. **9**, 2273 (2018).
[50] See Supplemental Material at http://link.aps.org/supplemental/10.1103/PhysRevB.107.L081302 for details of sample fabrication and characterization, experimental setup, and the theoretical approach.
[51] R. G. Stomphorst, G. van der Zwan, M. A. M. J. van Zandvoort, A. B. Sieval, H. Zuilhof, F. J. Vergeldt, and T. J. Schaafsma, J. Phys. Chem. A **105**, 4235 (2001).
[52] I. Carusotto and C. Ciuti, Rev. Mod. Phys. **85**, 299 (2013).
[53] A. Fetter and J. Walecka, *Quantum Theory of Many-Particle Systems*, Dover Books on Physics (Dover Publications, Mineola, N.Y., 1971).